

CHROM. 15,214

## HIGH-PERFORMANCE LIQUID CHROMATOGRAPHY USING FLEXIBLE FUSED-SILICA MICRO-PACKED COLUMNS

DAIDO ISHII and TOYOHIDE TAKEUCHI\*

*Department of Applied Chemistry, Faculty of Engineering, Nagoya University, Chikusa-ku, Nagoya-shi 464 (Japan)*

---

### SUMMARY

High-resolution flexible fused-silica micro packed columns were prepared by coupling 50-cm columns in series. These columns produced large numbers of theoretical plates (more than 100,000) and were successfully applied to the separations of epoxy oligomers and polychlorobiphenyl mixtures in gel permeation chromatography and reversed-phase liquid chromatography, respectively.

---

### INTRODUCTION

For the analysis of complex mixtures in the environment or *in vivo*, high-resolution columns producing more than 100,000 theoretical plates, as well as the optimization of operating conditions, are required. Greater numbers of theoretical plates are generally achieved with longer columns, however, the resulting large pressure drop generates heat in the column, which sometimes causes a reduction in column efficiency in conventional high-performance liquid chromatography (HPLC).

Scott and Kucera<sup>1-3</sup> prepared long microbore columns exhibiting large numbers of theoretical plates by coupling up to fourteen columns (0.5–1 m × 1 mm I.D.) in series, and reported that the heat problem could be eliminated by use of such columns.

We have also examined micro-HPLC. Specific injection, detection and column preparation techniques accompanied by miniaturization of HPLC have been discussed and demonstrated<sup>4</sup>. The use of fused-silica tubing as the column material in micro-HPLC has also been reported<sup>5,6</sup>. Such columns have high efficiencies due to their inert and smooth surfaces. They are also very easy to handle and facilitate the adjustment of coil diameter in long columns owing to their flexibility and mechanical strength. In the first work using fused-silica packed columns<sup>5</sup>, values on the height equivalent to a theoretical plate (HETP) of 14–20  $\mu\text{m}$  were obtained with 5–30 cm columns packed with 5- $\mu\text{m}$  particles. In later work<sup>6</sup>, columns were coupled in series in order to attain higher efficiencies, and around 40,000 and 100,000 theoretical plates were produced in reversed-phase liquid chromatography (LC) and gel permeation chromatography (GPC), respectively.

In this study, high-resolution flexible fused-silica columns yielding more than

100,000 theoretical plates have been prepared and applied to the separations of complex mixtures.

## EXPERIMENTAL

Reagents were purchased from Wako (Osaka, Japan) or Tokyo Chemical Industry (Tokyo, Japan), unless otherwise noted.

The apparatus employed was nearly the same as previous work<sup>6</sup>. A LC pump was generally composed of a Micro Feeder (Azumadenki Kogyo, Tokyo, Japan) and a gas-tight syringe. A simple constant-pressure pump comprising a gas-tight syringe and a weight was also employed as the LC pump. The required pressure was attained by changing the weight and the dimensions of the gas-tight syringe, as described previously<sup>7</sup>, *e.g.*, 50 kg/cm<sup>2</sup> was attained by using a 5-kg weight and a 500- $\mu$ l gas-tight syringe. The sample was generally injected by a Micro Valve Injector (0.02  $\mu$ l; Jasco, Japan Spectroscopic, Tokyo, Japan). Stop-flow injection was also used.

Two types of fused-silica tubings are commercially available, *i.e.*, silicone-coated and polyimide-coated tubings. The latter is preferred as the column material in micro-HPLC owing to its lower solubility in organic solvents and greater heat-resistance. Therefore, in this work, polyimide-coated fused-silica tubings (0.25 and 0.35 mm I.D.) (Gasukuro Kogyo, Tokyo, Japan) were selected. The exact inside diameter was measured by microscopy.

Both ends of a fused-silica tubing were inserted into PTFE tubings (0.2 mm I.D., 2 mm O.D.) by using a micro burner and covered with larger-bore PTFE tubings triply in order to withstand high pressure. Packings employed were TSK-GEL G 1000H (5  $\mu$ m, exclusion limit  $1 \times 10^3$ ; Toyo Soda, Tokyo, Japan), G 3000H (5  $\mu$ m, exclusion limit  $6 \times 10^4$ ; Toyo Soda) and silica ODS SC-01 (5  $\mu$ m, JASCO). Solvents were carefully selected by considering the properties of both mobile and stationary phases employed, *e.g.*, tetrahydrofuran (THF) for GPC, a mixture of acetonitrile and toluene for reversed-phase LC, etc. The slurried packing solution was forced manually into the prepared fused-silica tubing by using a gas-tight syringe. Leakage was prevented by quartz wool. Columns were connected by stainless-steel tubing (4–5  $\times$  0.13 mm I.D., 0.31 mm O.D.). The connection volume was only 0.05–0.06  $\mu$ l and this system could withstand pressures of 80–100 kg/cm<sup>2</sup>.

## RESULTS AND DISCUSSION

In previous work<sup>5</sup> it was demonstrated that HETP was slightly dependent on mobile phase flow-rate, values between 13 and 20  $\mu$ m being obtained for a 10-cm column in reversed-phase LC. These results show that the packing is ideally performed and that the contribution of band broadening in the extra-column parts is negligibly small. Several 50-cm columns were prepared and their performance in modes such as GPC, reversed-phase LC, intermediate-phase LC and normal-phase LC was examined.

Figs. 1–4 show the relationships between mobile phase flow-rate and HETP. The mean particle diameter of all the packings is 5  $\mu$ m. The highest column efficiency was attained for reversed-phase LC, low HETP values of 14–19  $\mu$ m being observed. In intermediate-phase LC using G 1000H and diethyl ether as the stationary and the

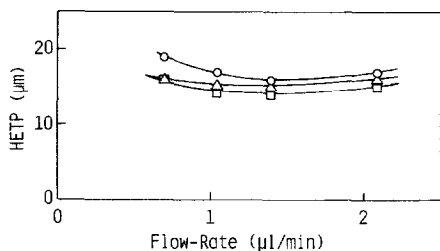


Fig. 1. Relationship between flow-rate and HETP for GPC. Column: TSK-GEL 3000H, 0.5 m  $\times$  0.33 mm I.D. Mobile phase: THF. Sample: benzene.

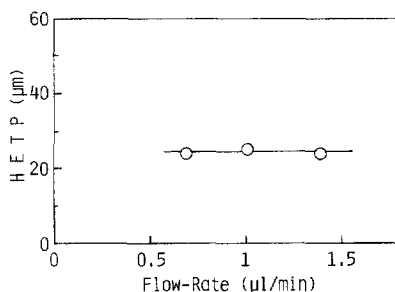


Fig. 2. Relationship between flow-rate and HETP for reversed-phase LC. Column: Silica ODS SC-01, 0.5 m  $\times$  0.26 mm I.D. Mobile phase: acetonitrile-water (8:2, v/v). Samples:  $\circ$ , benzene ( $k' = 0.48$ );  $\triangle$ , anthracene ( $k' = 1.98$ );  $\square$ , pyrene ( $k' = 2.91$ ).

mobile phases, respectively, the HETP was dependent on flow-rate and  $k'$ , whereas a weaker dependence was observed in the other modes. The mobile phases employed in the intermediate-phase and the normal-phase systems such as diethyl ether and *n*-butane have low viscosities, which will be advantageous for the operation of long columns. The apparatus using *n*-butane as the mobile phase was the same as in previous work<sup>8</sup>.

The dependence of column efficiency on solute retention is illustrated in Fig. 5. Nearly the same HETP values are obtained over the range  $k' = 0.5$ –3, indicating that the additional band broadening in the injection, connection and detection parts can be neglected for the system employed in this work.

Typical chromatograms obtained on 50-cm columns in the reversed-phase,

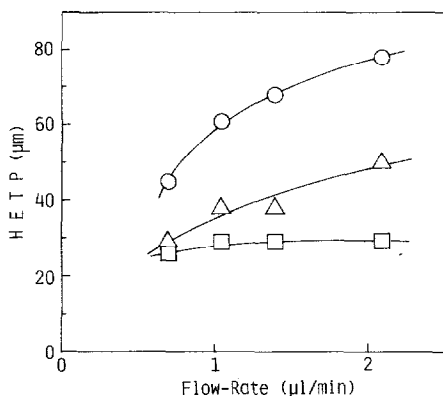


Fig. 3. Relationship between flow-rate and HETP for intermediate-phase LC. Column: TSK-GEL G 1000H, 0.5 m  $\times$  0.26 mm I.D. Mobile phase: diethyl ether. Samples:  $\square$ , benzene ( $k' = 0.13$ );  $\triangle$ , anthracene ( $k' = 0.67$ );  $\circ$ , 3,4-benzopyrene ( $k' = 1.59$ ).

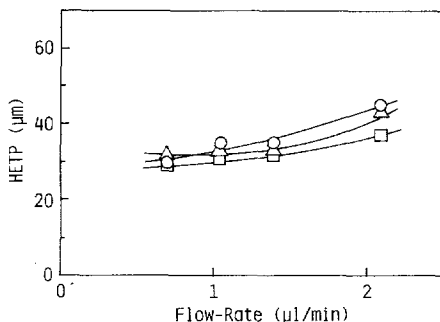


Fig. 4. Relationship between flow-rate and HETP for normal-phase LC. Column: Silica ODS SC-01, 0.5 m  $\times$  0.26 mm I.D. Mobile phase: *n*-butane. Samples:  $\square$ , anthracene ( $k' = 0.44$ );  $\triangle$ , chrysene ( $k' = 1.13$ );  $\circ$ , 3,4-benzopyrene ( $k' = 2.04$ ).

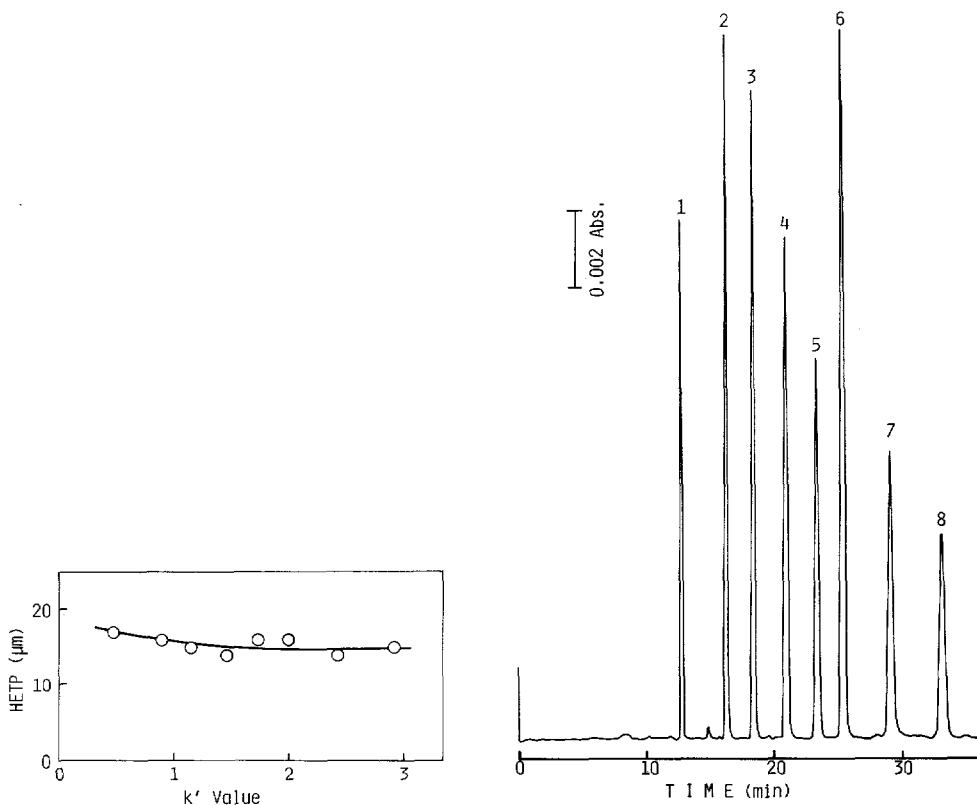


Fig. 5. Dependence of column efficiency on solute retention. Operating conditions as in Fig. 2 except for the samples: benzene; naphthalene; biphenyl; fluorene; phenanthrene; anthracene; fluoranthene; and pyrene; eluted in that order.

Fig. 6. Separation of polynuclear aromatic hydrocarbons in the reversed-phase mode. Column: Silica ODS SC-01, 0.5 m  $\times$  0.26 mm I.D. Mobile phase: acetonitrile-water (8:2 v/v). Flow-rate: 2.08  $\mu$ l/min. Samples: 1 = benzene; 2 = naphthalene; 3 = biphenyl; 4 = fluorene; 5 = phenanthrene; 6 = anthracene; 7 = fluoranthene; 8 = pyrene. Wavelength of UV detection: 254 nm.

intermediate-phase and normal-phase modes are shown in Figs. 6–8, respectively. 30,000–36,000 Theoretical plates are attained in the reversed-phase mode, as shown in Fig. 6.

50-cm columns were connected and the column performance was examined in GPC using G 3000H and THF as the stationary and the mobile phases, respectively. The relationship between column length and the theoretical plate number is illustrated in Fig. 9. More than 100,000 theoretical plates are attained on columns longer than 2 m.

These GPC columns were applied to the separation of epoxy oligomers, Epikote 828, 1001 and 1004. The structure of Epikote oligomers is illustrated in Fig. 10; the degree of polymerization and the distribution can be varied to suit the application.

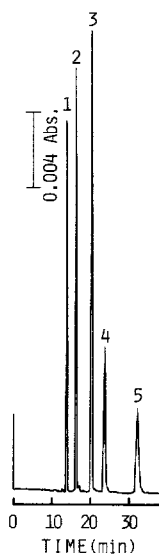


Fig. 7. Separation of polynuclear aromatic hydrocarbons in the intermediate-phase mode. Column: TSK-GEL G 1000H, 0.5 m  $\times$  0.26 mm I.D. Mobile phase: diethyl ether. Flow-rate: 1.39  $\mu$ l/min. Samples: 1 = benzene; 2 = naphthalene; 3 = anthracene; 4 = pyrene; 5 = 3,4-benzopyrene. Wavelength of UV detection: 254 nm.

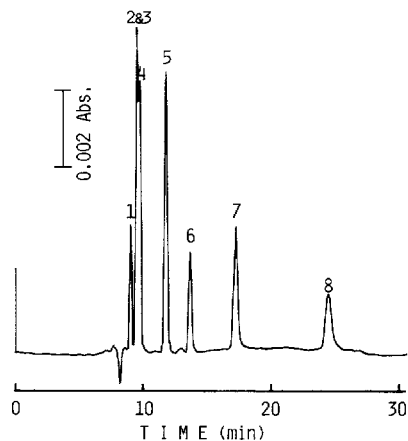


Fig. 8. Separation of polynuclear aromatic hydrocarbons in the normal-phase mode. Column: Silica ODS SC-01, 0.5 m  $\times$  0.26 mm I.D. Mobile phase: *n*-butane. Flow-rate: 2.08  $\mu$ l/min. Samples: 1 = benzene; 2 = naphthalene; 3 = biphenyl; 4 = 1,3,5-triphenylbenzene; 5 = anthracene; 6 = pyrene; 7 = chrysene; 8 = 3,4-benzopyrene. Wavelength of UV detection: 254 nm.

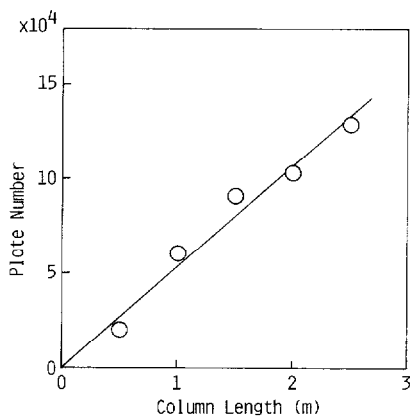


Fig. 9. Relationship between column length and the theoretical plate number. Column: TSK-GEL G 3000H. Mobile phase: THF. Flow-rate: 1.04  $\mu$ l/min. Sample: benzene.

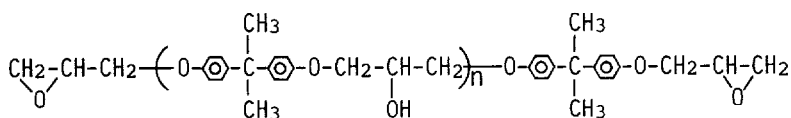


Fig. 10. The structure of Epikote oligomers.

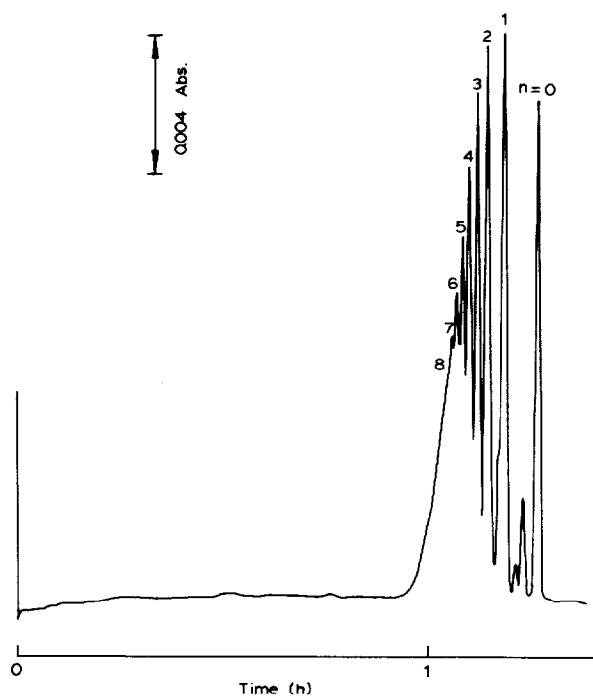


Fig. 11. Separation of Epikote 1001 on a 1.5-m  $\times$  0.33-mm column of TSK-GEL G 3000H. Mobile phase: THF. Flow-rate: 1.04  $\mu$ l/min. Sample: 0.02  $\mu$ l of 3.7% Epikote 1001 in THF. Wavelength of UV detection: 280 nm.

Figs. 11–13 show chromatograms of Epikote 1001 obtained on 1.5-m, 2.5-m and 4-m columns, respectively. Peaks corresponding to degrees of polymerization ranging from  $n = 0$  to  $n = 11$  can be observed for the 4-m column, as shown in Fig. 13. Two impurities are detected between the  $n = 0$  and  $n = 1$  peaks and some

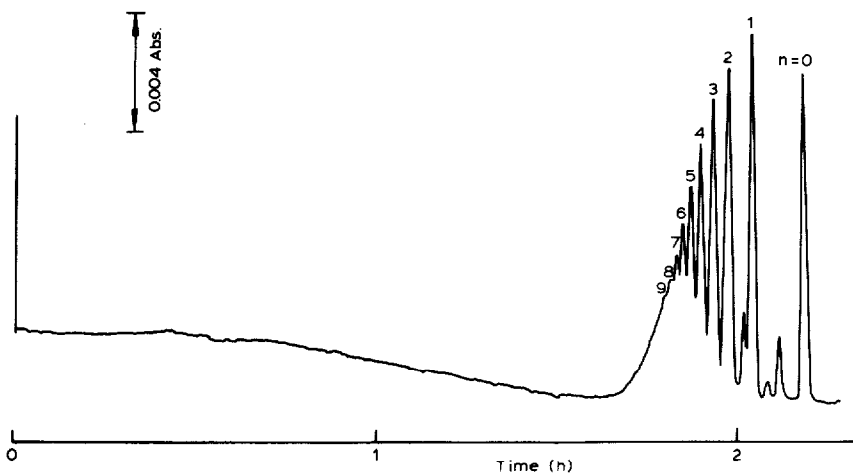


Fig. 12. Separation of Epikote 1001 on a 2.5-m column. Operating conditions as in Fig. 11 except the column length.

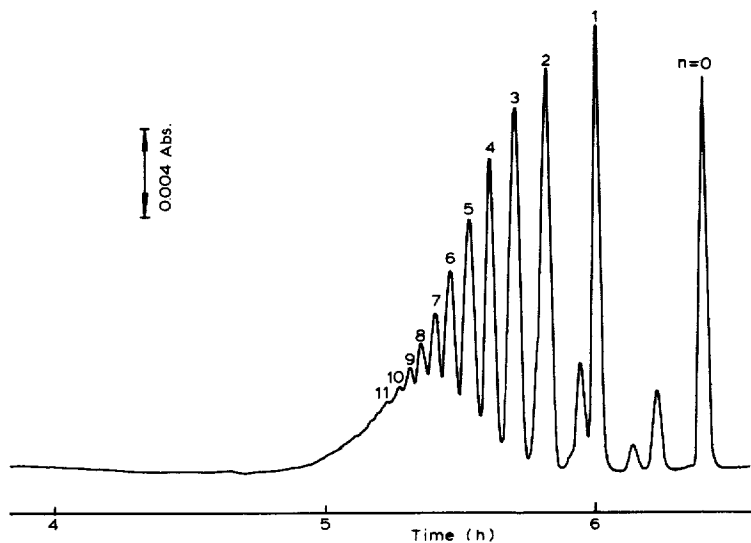


Fig. 13. Separation of Epikote 1001 on a 4-m column. Operating conditions as in Fig. 11 except as indicated. Flow-rate:  $0.56 \mu\text{l}/\text{min}$ . Sample:  $0.02 \mu\text{l}$  of 7.5% Epikote 1001 in THF.

impurities are found as shoulders also in other regions. High resolution is attained on a 4-m column and 230,000 theoretical plates are produced for a  $n = 0$  peak.

Figs. 14 and 15 show chromatograms of Epikote 1004 and 828 obtained on a 2.5-m column, respectively.

The molecular weight calibration plot for epoxy oligomers is shown in Fig. 16. A linear relationship between the logarithm of molecular weight and elution time is observed except for the  $n = 0$  peak.

The resolution of these micro-scale GPC columns is comparable to that of conventional GPC columns<sup>9</sup> whose cross-sectional areas are several hundred times larger. In other words, the consumption of both stationary and mobile phases can be remarkably reduced in micro-scale GPC, leading to high-resolution low-cost LC.

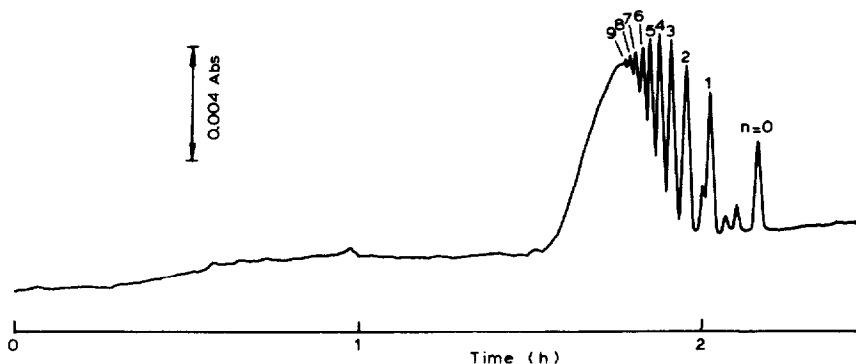


Fig. 14. Separation of Epikote 1004 on a 2.5-m column. Operating conditions as in Fig. 11 except as indicated. Sample:  $0.02 \mu\text{l}$  of 4.8% Epikote 1004 in THF.

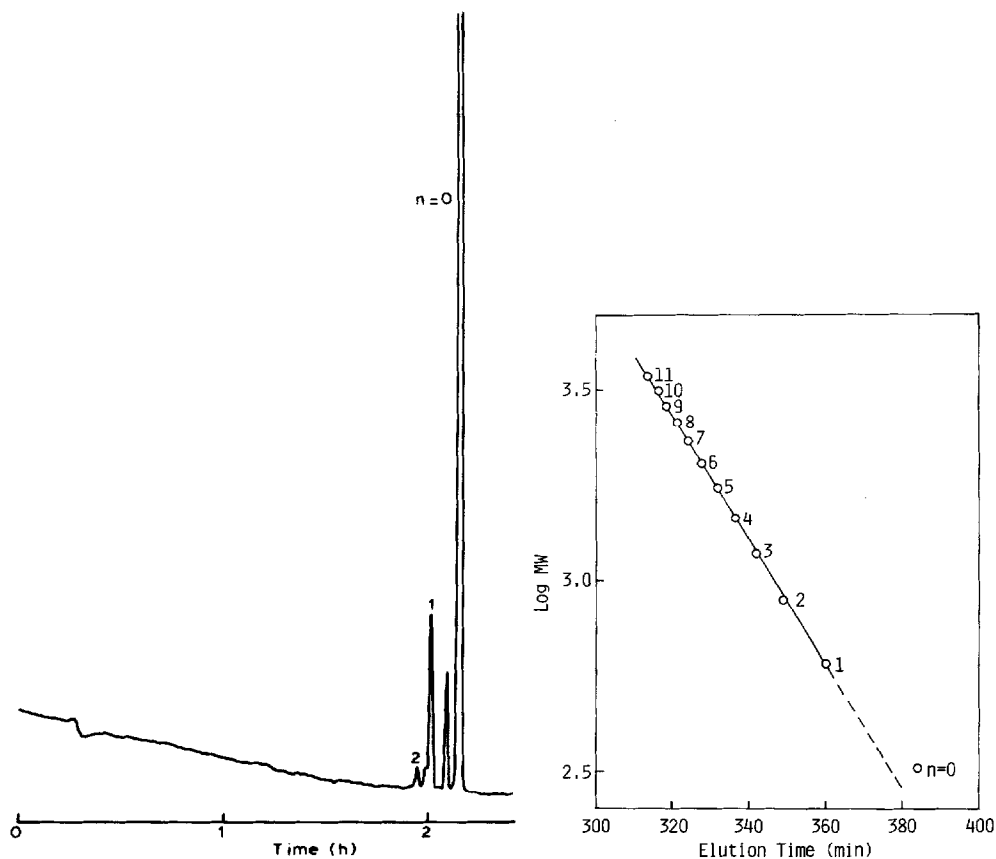


Fig. 15. Separation of Epikote 828 on a 2.5-m column. Operating conditions as in Fig. 11 except as indicated. Sample: 0.02  $\mu\text{l}$  of 4.3% Epikote 828 in THF.

Fig. 16. Molecular weight calibration plot. Column: TSK-GEL G 3000H, 4.0 m  $\times$  0.33 mm I.D. Mobile phase: THF. Flow-rate: 0.56  $\mu\text{l}/\text{min}$ . Sample: Epikote 1001.

Reversed-phase LC columns packed with ODS can exhibit high resolution. 1.5-m Columns were prepared and applied to the separations of polynuclear aromatic hydrocarbons and polychlorobiphenyl (PCB) mixtures. The chromatograms obtained are shown in Figs. 17 and 18. Many peaks are resolved in Fig. 18, owing to the high resolution of this column. These chromatograms were obtained by constant-pressure operation, as described in the Experimental section. Good results are obtained in spite of the simple pumping system.

## CONCLUSION

Flexible fused-silica micro packed columns coupled in series yielded high resolution. More than 100,000 theoretical plates were produced and successfully applied to the separations of complex mixtures.



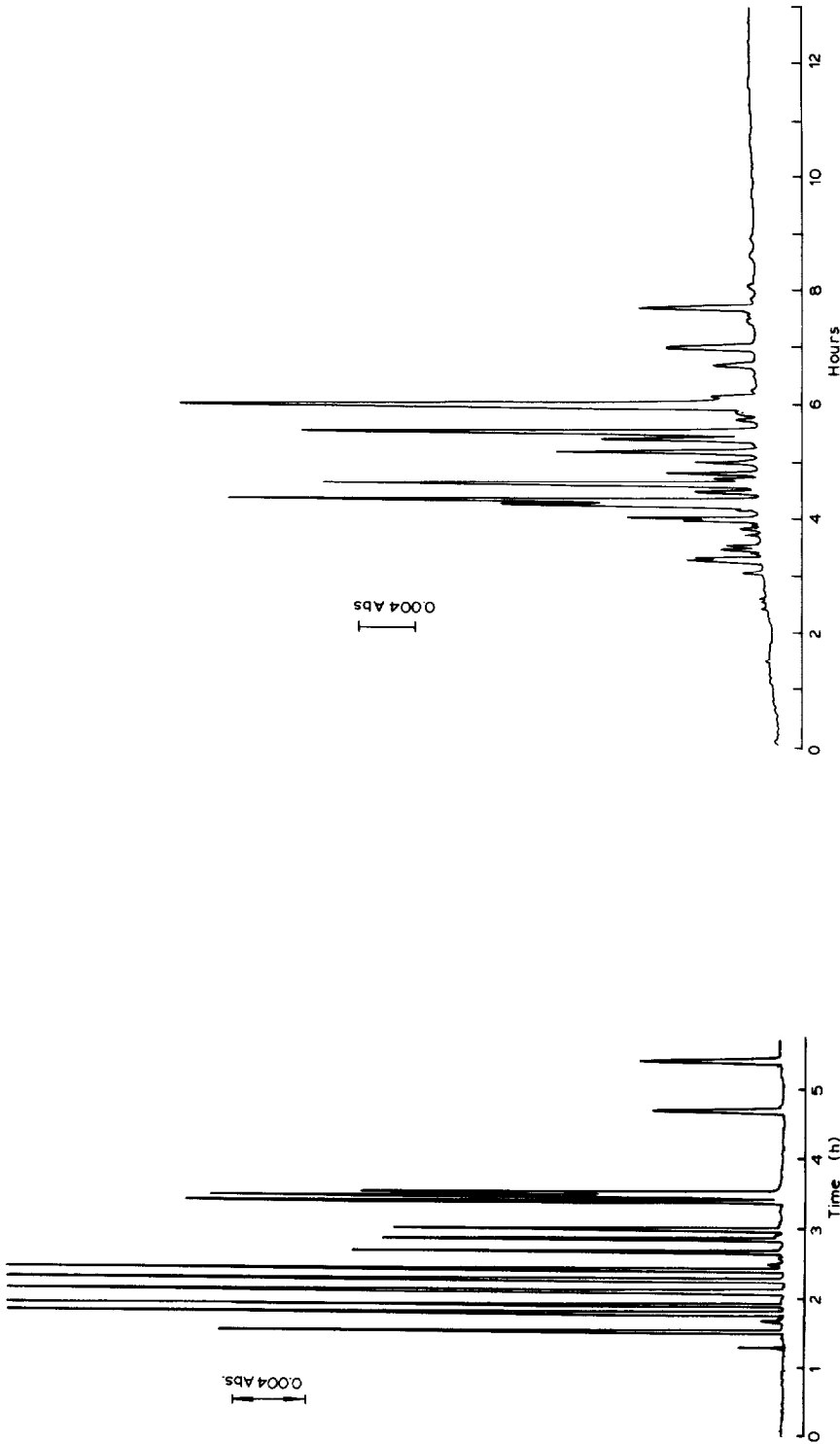


Fig. 17. Separation of polynuclear aromatic hydrocarbons in the reversed-phase mode. Column: Silica ODS SC-01, 1.5 m  $\times$  0.26 mm I.D. Mobile phase: acetonitrile-water (9:1). Inlet pressure: 50 kg/cm<sup>2</sup> (0.75  $\mu$ l/min). Sample mixture: benzene; naphthalene; biphenyl; fluorene; phenanthrene; anthracene; fluoranthene; pyrene; *p*-terphenyl; chrysene, 9-phenylanthracene; 1,3,5-triphenylbenzene; perylene and 3,4-benzopyrene. Injection volume: 0.2  $\mu$ l (by stop-flow injection). Wavelength of UV detection: 254 nm.

Fig. 18. Separation of PCB mixture on an ODS column. Column: Silica ODS SC-01, 1.5 m  $\times$  0.26 mm I.D. Mobile phase: acetonitrile-water (85:15 v/v). Inlet pressure: 50 kg/cm<sup>2</sup> (0.6  $\mu$ l/min). Sample: 0.02  $\mu$ l of 5.0% PCB-48 (chlorine content 48%) in acetonitrile. Wavelength of UV detection: 254 nm.

## ACKNOWLEDGEMENT

We wish to acknowledge Dr. Sadao Mori for his helpful suggestions.

## REFERENCES

- 1 R. P. W. Scott and P. Kucera, *J. Chromatogr.*, 125 (1976) 251.
- 2 R. P. W. Scott and P. Kucera, *J. Chromatogr.*, 169 (1979) 51.
- 3 R. P. W. Scott and P. Kucera, *J. Chromatogr.*, 185 (1979) 27.
- 4 D. Ishii, K. Asai, K. Hibi, T. Jonokuchi and M. Nagaya, *J. Chromatogr.*, 144 (1977) 157.
- 5 T. Takeuchi and D. Ishii, *J. Chromatogr.*, 213 (1981) 25.
- 6 T. Takeuchi and D. Ishii, *J. Chromatogr.*, 238 (1982) 409.
- 7 T. Takeuchi and D. Ishii, *J. Chromatogr.*, 239 (1982) 633.
- 8 T. Takeuchi, Y. Watanabe, K. Matsuoka and D. Ishii, *J. Chromatogr.*, 216 (1981) 153.
- 9 S. Ishiguro, Y. Inoue and T. Hosogane, *J. Chromatogr.*, 239 (1982) 651.